Electron dynamics of a two-dimensional electron gas with a random array of InAs quantum dots

S. Cinà
Cavendish Laboratory, University of Cambridge, Madingley Road, Cambridge, United Kingdom and Toshiba Research Europe Limited, 260 Science Park, Milton Road, Cambridge, United Kingdom

D. D. Arnone
Toshiba Research Europe Limited, 260 Science Park, Milton Road, Cambridge, United Kingdom

H. P. Hughes
Cavendish Laboratory, University of Cambridge, Madingley Road, Cambridge, United Kingdom

C. L. Foden and D. M. Whittaker
Toshiba Research Europe Limited, 260 Science Park, Milton Road, Cambridge, United Kingdom

M. Pepper
Cavendish Laboratory, University of Cambridge, Madingley Road, Cambridge, United Kingdom and Toshiba Research Europe Limited, 260 Science Park, Milton Road, Cambridge, United Kingdom

D. A. Ritchie
Cavendish Laboratory, University of Cambridge, Madingley Road, Cambridge, United Kingdom
(Received 20 May 1999)

We show that the presence of InAs dots embedded in a host GaAs quantum well containing a two-dimensional electron gas dramatically modifies the cyclotron resonance (CR). Far-infrared CR measurements show two modes with different dispersions with applied magnetic field *B*. The lower-frequency mode, with a sublinear dependence on *B*, is identified as a CR at low *B*, developing into a skipping orbit around the dot perimeters at higher *B*; this has not been previously observed for a system with randomly distributed scatterers. The higher-frequency mode is identified as a magnetoplasmon localized by the confining effect of the arrays of repulsive potentials due to the dots in the well. The linewidths of these modes, despite the broad size distribution of the dots, are narrow, suggesting that Coulombic interactions are important. [S0163-1829(99)02435-2]

The electrical and optical properties of a two-dimensional electron gas (2DEG) in the presence of various types of scattering centers have been well studied. Novel growth techniques[1] now allow mesoscopic structures such as charged quantum dots with small ($\sim$20 nm) radii to be incorporated directly into quantum wells (QW's) containing 2DEGs. The optical properties of the dots themselves, such as strong zero-dimensional confinement,[2] have been extensively studied and manipulated for potential devices.[3] But, although scattering by self-organized InAs dots in GaAs QW's has been suggested as limiting the mobility of a 2DEG in the host QW,[4] little work has been done on the effects of the dots on the optical properties of the host 2DEG itself. Far-infrared (FIR) cyclotron-resonance (CR) spectroscopy is an excellent probe of many relevant properties, revealing distinct signatures of confinement in dots,[5] antidot behavior,[6] impurity bound electrons,[7] and other phenomena.

In the absence of impurities or other potential fluctuations in or near the QW which destroy its in-plane translational invariance, a single CR absorption mode is observed, and Kohn's theorem[8]—that the collective excitation spectrum consists of a single mode associated with the center-of-mass motion and which is unaffected by electron-electron interactions—accurately describes the absorption. Here, self-organized InAs dots are introduced into a GaAs QW, breaking the translational invariance of the 2DEG and splitting the CR mode into two modes with different dispersions with magnetic field *B*. The effects observed are distinct in important respects from previous work in which charged impurities were placed close to the QW,[9,10] in that one mode shows a clear sublinear dependence on *B* and the two modes show a strongly different carrier density dependence.

The samples were fabricated on an undoped (100) GaAs substrate by first growing 600 nm of GaAs at 580 °C, followed by a 50 nm undoped $Al_xGa_{1-x}As$ barrier, a 30 nm GaAs QW, a 40 nm undoped $Al_xGa_{1-x}As$ spacing layer, a 40 nm Si-doped (1×10^{18} cm^{-3}) $Al_xGa_{1-x}As$ layer, and a 17 nm GaAs capping layer. A semitransparent ($\sim$7 nm) NiCr gate on top of the structure allowed control of the 2DEG carrier density N_s. Following the Stranski-Krastanov technique,[1] 2.0 monolayers (ML) of InAs were grown in the QW, on top of the first 10 nm of GaAs, at 530 °C. A 10 nm GaAs layer was also grown at this temperature to protect the InAs when the temperature was returned to 580 °C to grow the remaining layers. Several samples (*a*, *b*, and *c*) with different dot densities (N_d) were studied. N_d, averaged over a large area (12 μm^2), were measured directly for samples *a* and *b* using transmission electron microscopy (TEM):[11] for sample *a* from the center of a wafer, $N_d\simeq5.8\times10^9$ cm^{-2}, and for *b* from midway between the center and the edge of

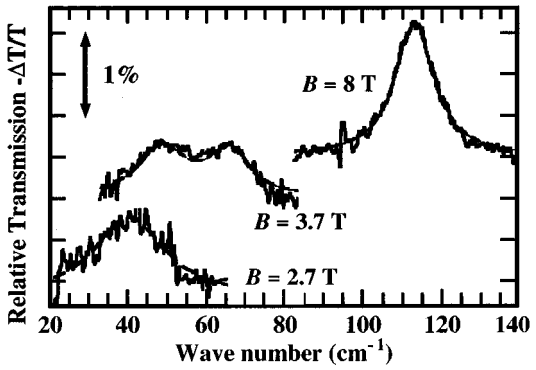

FIG. 1. Relative transmission measured for sample *a* at different *B*. Dotted lines are Lorentzian fits.

the wafer, $N_d \simeq 4.6\times10^9$ cm^{-2}. Sample *c* was from a different wafer which included 2.8 ML of InAs covered with a 1-nm-thick GaAs capping layer. This capping layer, thinner than for samples *a* and *b*, implies that sample *c* should include 1-nm-high dots. The dot diameter should also be ~30% larger than for samples *a* and *b* because of the 2.8 ML InAs thickness.[12] The TEM images of the same samples[11] show well defined dots ~33 nm in diameter in sample *a*; a dot height ~8 nm was estimated from a cross-sectional TEM image.

Magnetotransport and FIR CR measurements (using a Fourier transform spectrometer) were performed at 3.3 K using a 4 mm^2 Hall bar on a wedged substrate (5°) to avoid interference effects. N_s at different gate biases (V_g) were estimated from Shubnikov–de Haas measurements. The relative FIR transmission $[-\Delta T/T = 1 - T(B)/T(B=0)]$ measured for a reference sample containing no InAs dots showed a single CR peak with a frequency well described by $\omega_c = eB/m^*$ (with $m^* = 0.070 m_e$, e the electronic charge and m_e the free-electron mass), as expected.

Similar FIR measurements were made for samples *a*, *b*, and *c*. Figure 1 shows spectra for $N_s = 2.6\times10^{11}$ cm^{-2} at various *B* for sample *a*, and Figs. 2 and 3 show the CR peak position versus *B* for all samples. A single peak is observed for $B \leqslant 2.7$ T and $B > 4.6$ T for sample *a* ($B \leqslant 3$ T and $B > 5.5$ T for *b*, $B \leqslant 4.2$ T and $B > 7.2$ T for *c*), while at intermediate fields two peaks are observed. The intensities of these peaks—proportional to the number of electrons involved in each transition—change markedly with *B*. For sample *a*, the higher-frequency mode is first observed at $B = 3.2$ T, and its intensity is ~30% that of the lower mode. The intensities become equal around $B = 4$ T, and at $B = 4.6$ T, when the lower mode is last observed, the intensity of the higher mode is three times that of the lower. Similar behavior occurs for samples *b* and *c*. The frequencies of the lower modes in each sample lie below the CR line, and, as most clearly shown in sample *c*, they also vary sublinearly with *B*.

The immediate impression from Figs. 2 and 3 is that there is an anticrossing between ω_c and some optically inactive mode ω_m. But it is clear that ω_m must disperse upwards with *B* with a gradient less than that of ω_c. Whatever ω_m might be, this would require that the effective electron mass involved exceeds the usual cyclotron mass (in fact, $m_m^* = 0.11 m_e^*$). No such mode can be accounted for, and the interpretation of the two branches must be sought elsewhere.

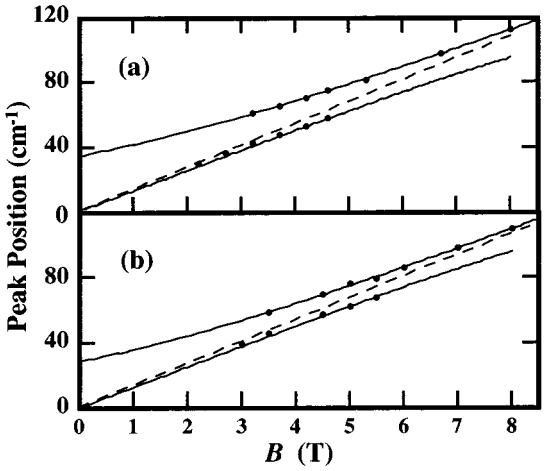

FIG. 2. Measured peak positions vs *B* for samples *a* and *b*. The data dot size reflects the energy error bar. The continuous lines are fits with the solutions of Eq. (1) for the low-frequency branches and with ω_+ from Eq. (3) for the high-frequency branches. The dashed line shows the CR measured on the reference sample.

Because of their lower conduction-band minima, the InAs dots, coexisting with the 2DEG, must be negatively charged;[13] this results in a repulsive potential around each dot,[4] and corresponding potential fluctuations in the plane of the 2DEG, for which the InAs inclusions therefore have *antidot* electrostatic characteristics, and it is natural to look to antidotlike phenomena to explain our observations.

This random array of repulsive centers in the QW can give rise to two types of electron motion in the presence of *B*—skipping orbits around individual repulsive centers[14], and a collective motion effectively confined in ''corrals'' by the surrounding repulsive centers (Fig. 4). The latter behavior has been observed for a GaAs-$Al_xGa_{1-x}As$ QW with a nearby δ-doped negatively charged acceptor (Be) layer[9] and discussed theoretically by Merkt[15] (see below). These behav-

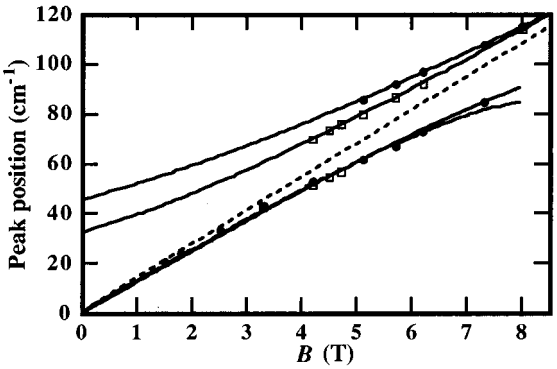

FIG. 3. Measured peak positions vs *B* for sample *c*. The data dot size reflects the energy error bar. The continuous lines are fits with the solutions of Eq. (1) for the low-frequency branches and with ω_+ from Eq. (3) for the high-frequency branches. Dots correspond to $N_s = 2.6\times10^{11}$ cm^{-2} and squares to $N_s = 2.0\times10^{11}$ cm^{-2}. The dashed line shows the CR measured on the reference sample. The lower-frequency modes have clear sublinear dependences on *B*.

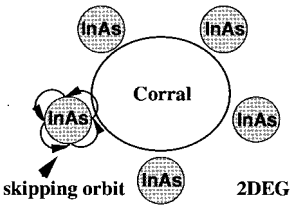

FIG. 4. Schematic of the skipping orbits, and a confining ''corral.''

iors are in some sense similar, in that the electron orbits scatter from repulsive centers, but since no theoretical description satisfactorily covers both, we therefore separate the discussion for the lower- and higher-frequency modes observed.

The lower branch can be explained in terms of antidotlike behavior. At low B, when the cyclotron radius R_c is greater than the InAs dot radius R_d, a simple CR mode is observed. With increasing B, R_c becomes comparable with R_d and the mode evolves into a skipping mode around a dot (Fig. 4). As for the antidot systems in which such skipping orbits have been observed,[6] the mode energy increases sublinearly with B (i.e., with decreasing R_c) and decreases in intensity, until a critical value is reached beyond which the mode shows a downturn and negative dispersion with B. This value depends on R_d as well as on N_d, and is characterized by a spatial filling factor f, the ratio between the area covered with dots and the total sample area, used in effective medium approximation (EMA) calculations of the energy dispersion (ω versus B).[16,17] The mode dispersions for an antidot system in such an EMA are obtained from[16]

$$1-\frac{1-f}{\Omega(\Omega+\Omega_c)}-\frac{f}{\Omega(\Omega-\Omega_c)}=0, \tag{1}$$

where $\Omega=\omega/\omega_1$ and $\Omega_c=\omega_c/\omega_1$, and

$$\omega_1=\sqrt{\frac{3\pi^2 N_s e^2}{8m^*\epsilon_0\epsilon_{\rm eff}R_d}}. \tag{2}$$

Equation (1) and other EMA calculations[17] give three branches, the lowest of which disperses initially sublinearly with B as observed experimentally; it eventually shows the downturn and negative dispersion with B expected for edge-magnetoplasmon modes, but the antidot sizes and the magnitude of B available here did not allow this to be observed. Equation (1) was used to fit the lower frequency branches in Figs. 2 and 3, and gave $R_d=25$ nm and $f=0.03$ for sample a, $R_d=25$ nm and $f=0.025$ for b, $R_d=33$ nm and $f=0.04$ for c. These results are consistent with the values of R_d and N_d obtained from the TEM images for samples a and b,[11] and with the larger R_d (and consequent increase in f) expected for sample c because of the thicker InAs layer used during its growth.[12] The larger value of $R_d=25$ nm obtained by the fits, compared with that observed in the TEM images[11] ($R_d\simeq 17$ nm), may be due to lateral depletion effects around the edge of InAs dots as well as to a larger ''antidot'' radius felt by the skipping electrons in the 2DEG. The more pronounced sub-linear behavior observed for sample c is attributable to its larger value of R_d producing the transition to a skipping mode at lower B.

The validity of this antidot model is also confirmed by demonstrating that the lower mode follows the N_s dependence in Eq. (1) and Eq. (2). Reducing N_s to 2.0×10^{11} cm^{-2} markedly reduces the range of B in which the low-frequency branch can be observed, as shown in Fig. 3 for sample c. Then a fit with Eq. (1) is too imprecise, but the lower branch of Eq. (1) can be drawn by using the same values of f and R_d obtained for $N_s=2.6\times10^{11}$ cm^{-2}, but changing N_s in Eq. (2). Figure 3 shows that the low-frequency branch should be roughly unaffected by the change in N_s in the observed range of B, consistent with our data.

The higher frequency branch of Eq. (1) corresponds at high B to CR motion between the antidots,[14] and at lower B shows a negative dispersion with B. This mode has been observed in square arrays of antidots, and attributed[14] to a one-dimensional (1D) edge magnetoplasmon propagating along the regular rows. This picture obviously cannot be applied to our devices, where the InAs dots are irregularly distributed; indeed, our experimental high-frequency branches cannot be realistically fitted with the higher-frequency modes from Eq. (1). However, since the low-frequency branch corresponds to electrons skipping around individual antidots, it is relatively unaffected by the irregularity of the antidot distribution and can be fitted quite well with Eq. 1.

To explain the higher-frequency branch, we note that the CR resonance was split by ~ 20 cm^{-1} for a GaAs-$Al_xGa_{1-x}As$ QW with a δ-doped (Be) acceptor layer nearby.[9] These acted as repulsive centers, and the potential fluctuations in the QW constrained the 2DEG in ''puddles'' to produce a confined collective mode. This picture was supported by the theoretical discussions of Merkt,[15] who noted that the new CR modes mark a departure from Kohn's theorem and have a B dispersion of the same form as for a 2DEG confined in zero dimension.[5] A similar interpretation can be applied to the repulsive centers in the InAs/GaAs system here. TEM images[11] show that the distribution of InAs dots is not completely random, but regions of the 2DEG—corrals—are loosely enclosed by more closely spaced dots. The high-frequency data can then be fitted using the upper branch (+) of the dispersion relation for the collective modes of a 2DEG confined in all three dimensions,[5] which is also valid for confinement by randomly distributed centers:[15]

$$\omega_{\pm}=\pm\frac{\omega_c}{2}+\sqrt{\left(\frac{\omega_c}{2}\right)^2+\omega_0^2}, \tag{3}$$

where ω_0 is the magnetoplasmon frequency at $B=0$, given by[5]

$$\omega_0=\sqrt{\frac{0.81N_s e^2}{2m^*\epsilon_0\epsilon_{\rm eff}R}}, \tag{4}$$

where $2R$ is the overall size of the corral and $\epsilon_{\rm eff}$ ($=12.5$) is the effective dielectric constant. Fitting the higher-frequency mode data with Eq. (3) gives $\omega_0=35$ cm^{-1} for sample a, 29 cm^{-1} for sample b, and 45 cm^{-1} for sample c, corresponding to confinement dimensions $2R=180$, 260, and 140 nm, respectively. These agree well with the average corral

dimensions (150–200 nm for sample *a* and 250–300 nm for *b*), and with those estimated for sample *c* from the different dot dimensions.[12]

Measurements were also made for various N_s, modified by V_g. Fitting the high-frequency branches with Eq. (3) gave values of ω_0 which decreased with decreasing N_s as shown in Fig. 3, and consistent with Eq. (4).

In previous CR studies on 2DEG's in the presence of negatively charged acceptors,[9,10] positively charged donors,[9] random potential fluctuations in high mobility samples,[18] or in Si-based systems,[19] the observed peaks were ascribed to localized modes arising from the confinement effects of the impurity-induced potential fluctuations as observed here, and the B dispersions explained[15] by the ω_+ branch of Eq. (3). The ω_- mode of Eq. (3), corresponding to an edge magnetoplasmon skipping along the inside of the confining potential—the corral in this case—and which decreases in frequency and intensity for increasing B, was, as here, not observed. The CR-like mode which was observed may correspond to the low-frequency branch seen here, but with a sublinear dependence on B which could not be differentiated from linear behavior because of the smaller effective R_d for charged impurity atoms.

Although two modes have previously been observed in samples with embedded negatively charged impurities,[9,10] our measurements of the sublinear dispersion of the low-frequency mode, and the different N_s dependence of the two modes, allow a clear identification of the two modes.

So, we conclude that the overall repulsive potential of the InAs dots results in two modes: skipping orbits around individual dots with antidotlike dispersion and confinement of the collective electron motion by corrals of dots. Figures 2 and 3 suggest that their oscillator strengths are nonnegligible only when their energies lie close to ω_c, possibly because the random array of dots seriously scatters the overall motion except when the orbits are close to the CR.

Further, the interaction between corrals appears to be very important. Despite large variations in the overall corral dimensions R,[11] the two peaks observed at $B=3.7$ T have comparable linewidths (Fig. 1). Since the broadening of the low-frequency peak reflects the small variations in the individual dot dimension R_d,[11] this suggests that inhomogeneous broadening by the larger variations in the overall corral dimensions R due to the irregular spatial distribution of the dots is also not significant. Merkt[15] also noted that strong Coulombic interactions between adjacent corrals smooth the local potential, resulting in a single narrow peak at a mean value of ω_0 in Eq. (4).

In conclusion, GaAs QW's with embedded InAs quantum dots of different dimensions and densities show two FIR absorption modes with different energy dispersions versus B. The higher-frequency mode behaves like a magnetoplasmon, localized by the potential fluctuations introduced by the InAs dots. The lower-frequency mode is a CR mode at low B, and evolves into a skipping orbit around the dots for increasing B, as previously observed in antidot systems. It appears that InAs dots in an *n*-type QW act as repulsive centers for the host 2DEG, and that, for these large diameter ($\sim$30 nm) scatterers, electron trajectories corresponding to both dot and antidot behavior have been simultaneously observed. The importance of Coulombic interactions in mediating localization and scattering has also been suggested.

We are grateful to J. Singleton, D.S. Kainth, G.D. Lian, J. Yuan, and L.M. Brown for valuable discussions.

[1] J. M. Gerard, in *Confined Electrons and Photons*, edited by E. Burstein and C. Weisbuch (Plenum Press, New York, 1995), p. 357.
[2] M. Fricke *et al.*, Europhys. Lett. **36**, 197 (1996).
[3] K. Imamura *et al.*, Jpn. J. Appl. Phys., Part 1 **43**, 1445 (1995).
[4] E. Ribeiro *et al.*, Phys. Rev. B **58**, 1506 (1998).
[5] D. Heitmann *et al.*, Surf. Sci. **267**, 245 (1992).
[6] K. Kern *et al.*, Phys. Rev. Lett. **66**, 1618 (1991).
[7] J. P. Cheng, Y. J. Wang, B. D. McCombe, and W. Schaff, Phys. Rev. Lett. **70**, 489 (1993).
[8] W. Kohn, Phys. Rev. **123**, 1242 (1961).
[9] J. Richter, H. Sigg, K. V. Klitzing, and K. Ploog, Phys. Rev. B **39**, 6268 (1989).
[10] H. Sigg, D. Weiss, and K. V. Klitzing, Surf. Sci. **196**, 293 (1988).
[11] G. H. Kim *et al.*, Appl. Phys. Lett. **73**, 2468 (1998).
[12] J. M. Moison *et al.*, Appl. Phys. Lett. **64**, 196 (1994).
[13] M. Sato and Y. Horikoshi, Appl. Phys. Lett. **56**, 1555 (1990).
[14] D. Heitmann and J. P. Kotthaus, Phys. Today **46**(6), 56 (1993).
[15] U. Merkt, Phys. Rev. Lett. **76**, 1134 (1996).
[16] S. A. Mikhailov and V. A. Volkov, Phys. Rev. B **52**, 17 260 (1995).
[17] D. S. Kainth (private communication).
[18] R. J. Nicholas *et al.*, Phys. Rev. B **39**, 10 955 (1989).
[19] J. P. Cheng and B. D. McCombe, Phys. Rev. B **44**, 3070 (1991).